

Adsorption property and kinetic studies of activated carbon fibers prepared from tissues by CO₂ activation

Z. J. Zhang^{a,*}, J. Li^b, Z. Q. Li^a, B. L. Li^c, N. N. Xing^b

^aAnhui Conch Design and Research Institute of Building Materials Co., Ltd., Wuhu 241070, China

^bSchool of Materials Science and Engineering, University of Jinan, Jinan 250022, China

^cFaculty of Architecture Civil Engineering, Huaiyin Institute of Technology, Huai'an 223001, China

Well-developed micro and mesoporous activated carbon fibers (ACFs) with fiber structure were prepared from tissue by CO₂ activation. The XRD patterns and Raman spectrum indicated ACFs had a graphitic and amorphous structure. The SEM results indicated that the sample exhibited fiber structure with lots of mesoporous, with an average pore size of 2-5 nm. The specific surface area of 1517 m²/g, micro surface area of 412.9 m²/g, and total pore volume of 1.194 cm³/g were obtained at 900°C with CO₂ activation for 2 hours. ACFs showed relatively high methylene blue adsorption properties with an equilibrium adsorption capacity of 526 mg/g. The kinetic model of the Pseudo-second-order equation was more suitable for MB adsorption than the Pseudo-first-order equation and Intraparticle diffusion kinetics, with a high correlation coefficient value ($R > 0.999$). The present research provided a new idea of bionics for the manufacture of ACFs and brought forward a creative prospect for achieving energy-related CO₂ emissions to net-zero and mitigating global warming.

(Received July 3, 2023; Accepted October 10, 2023)

Keywords: Activated carbon fibers, Tissues, Microstructure, Adsorption kinetic, Methylene blue

1. Introduction

Activated carbon fibers (ACFs) show important advantages compared to conventional activated carbons. Smaller fiber diameters minimize diffusion limitations and allow rapid adsorption/desorption. It has a more concentrated pore size distribution and excellent adsorption capacity at low concentrations of adsorbent, with a large specific surface area, special surface reactivity, and ease of synthesis in the form of felts and cloths[1]. So it has been extensively applied in the fields of adsorption, separation, and catalysis, such as removing hazardous components in the exhaust gas, purifying drinking water, or treating wastewater[2-3]. Generally, polyacrylonitrile fiber[4], phenolic resin[5], pitch fiber[6], and viscose fiber[7] can be used as a

* Corresponding author: zzzj-ujn@163.com
<https://doi.org/10.15251/DJNB.2023.184.1213>

precursor to produce ACFs. However, these raw materials are mostly derived from petrochemical products, the manufacturing process is more complicated and the price of ACFs is higher, which leads to high production costs and aggravates the consumption of petroleum resources. Lignocellulosic materials are good and cheap carbonaceous precursors for the production of activated carbon. Consequently, more and more researchers are focusing on finding low-cost and green raw materials for the preparation of ACFs. In recent years, ACFs have been successfully prepared from some bio-resources such as liquefied wood[8], flax[9], coconut fibers[10], sisal[11], kenaf[12], and *Senegalia catechu*[13]. However, there are few reports on the preparation of ACFs from plant pulp fibers. Compared with natural templates such as wood and plant leaves, tissues, as the plant pulp fibers of mature industrial products, have properties such as stable composition (mainly contains C and O), porosity, density, wide sources, and low price[14]. These properties of tissues and the structure of cellulose fibers will be useful in activated carbon fiber production.

In general, activated carbon fibers exhibit different porosities and pore structure characteristics under various activation methods and treatment conditions. Activated carbon materials can be produced by physical or chemical activation. Chemical activation has been successfully applied to produce activated carbon using various chemical reagents, i.e., $ZnCl_2$ [15], H_3PO_4 [16], HCL[17], and KOH[18]. The Physical activation consists of two steps, one is the carbonization of the starting material, and the other is the activation of the char by using carbon dioxide[19] or steam. Carbon dioxide (CO_2) is a commonly used and effective activator for the activation techniques of ACFs since it is clean, cheap, easy to obtain, and facile to control. At the same time, CO_2 emissions to the atmosphere have resulted in several global environmental impacts, such as global climate change and global warming, which have become big issue in front of researchers. Many countries have announced pledges to achieve net-zero emissions over the coming decades to bring global energy-related CO_2 emissions to net zero by 2050. Currently, there is high interest in studies of CO_2 capture from the exhaust by adsorption on porous carbonaceous or non-carbonaceous materials. ACFs have been considered potential candidates for CO_2 capture. The recent research results show that ACFs activated by CO_2 have a more abundant micro-and mesoporous structure and have a better adsorption effect on CO_2 [20-22]. In addition, more interesting points are that in the CO_2 -activated process, CO_2 is reacted and the by-product contained CO and H_2 , which can be used as an alternative fuel in industry, such as cement clinker production. Figure 1 shows the CO_2 cycle by the CO_2 activation process.

In the present study, ACFs were directly produced by physically activating tissues with CO_2 , and their textural properties and adsorption capacity for methylene blue were characterized. The kinetic data of the adsorption process of methylene blue molecules on the prepared activated carbon fibers were also studied. It can provide a new idea of bionic for the manufacture of activated carbon fibers, meanwhile, bringing forward a creative assumption and prospect for mitigating global climate change.

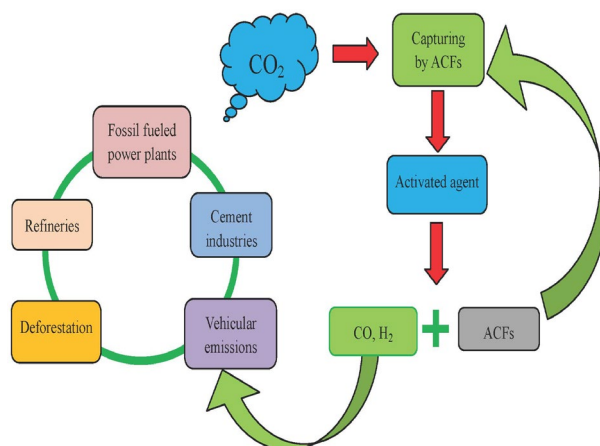


Fig. 1. CO₂ cycle by CO₂ activation process.

2. Materials and methods

2.1. Reagents and materials

The tissues (JiNan, China) were selected as a precursor of activated carbon fiber in this work. The preparation of the activated carbons fibers from tissues was carried out in Figure 2. The tissue was cut into square specimens of 2 cm×2 cm before carbonization and activation. The samples were firstly carbonized in a tube furnace under nitrogen (N₂) flow at 900 °C for 30 min at a heating rate of 5 °C /min, then the N₂ flow was turned off, and then the CO₂ flow (20 mL/min) was turned on. The char was activated by CO₂ at 900 °C for 1h, 2h, 3h, and 4h, respectively, to prepare the activated carbon fibers. The activated sample was washed several times with distilled water until the pH of the filtrate became neutral. The washed samples were dried at 60 °C for 12 h to prepare the activated carbon fibers.

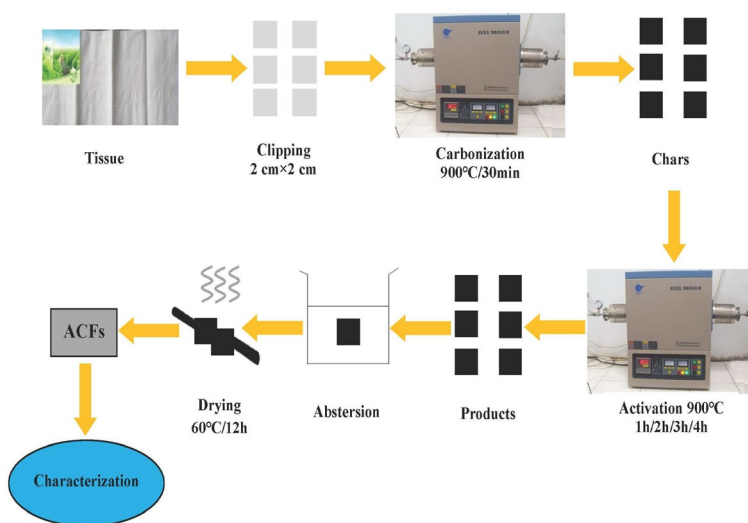


Fig. 2. The preparation process of activated carbon fibers from tissues by CO₂ activation.

2.2. Characterization

The phases of ACFs were analyzed by using an X-ray diffractometer (XRD with Cu-K α radiation source; Model D8-Advance, Germany) operated at 40 kV and 100 mA. A scanning electron microscopy (SEM; Model S-2500, Hitachi, Japan) equipped with an energy-dispersive X-ray spectrometer (EDS; Model INCA Energy 3294, Oxford, U.K.) was used to characterize the morphology and chemical composition of the samples. The specific surface area and pore volume of the samples were obtained by N₂ adsorption at 77 K with a Micromeritics ASAP 2020M+C system.

2.3. Adsorption kinetic experiments

Adsorption kinetic experiments were carried out in a glass vessel with 200 ml methylene blue (10 mg/L MB) and 4mg of ACFs at 25 °C. The recording time was started when ACFs were added to the vessel. Aqueous samples (3 ml) were taken from the solution at preset time intervals and the concentrations were analyzed by using a visual spectrophotometer (Model 722, Shanghai Jinghua, China) at 664 nm for methylene blue. The adsorption capacity time t , q_t (mg/g) was calculated by $q_t = V(C_0 - C_t)/W$, where C_0 and C_t were the liquid concentrations at the start time and at time t , respectively, and V was the volume of aqueous solution and W was the mass of ACFs.

3. Results and discussion

3.1. Characterization of ACFs

Figure 3 showed a typical SEM micrograph and EDS spectrum of the pure tissue used as the carbonaceous precursors in this paper. It revealed that the tissue contained a network of cellulose fibers with a diameter of about 20~25 μm . The cellulose-fiber structure of tissue led to the idea of using it to make ACFs. The EDS spectrum (inset Fig. 3(b)) and Table 1 confirmed that C and O were mainly present in the fibers (where Au is SEM conducting film), which helped to increase the amount of prepared carbon.

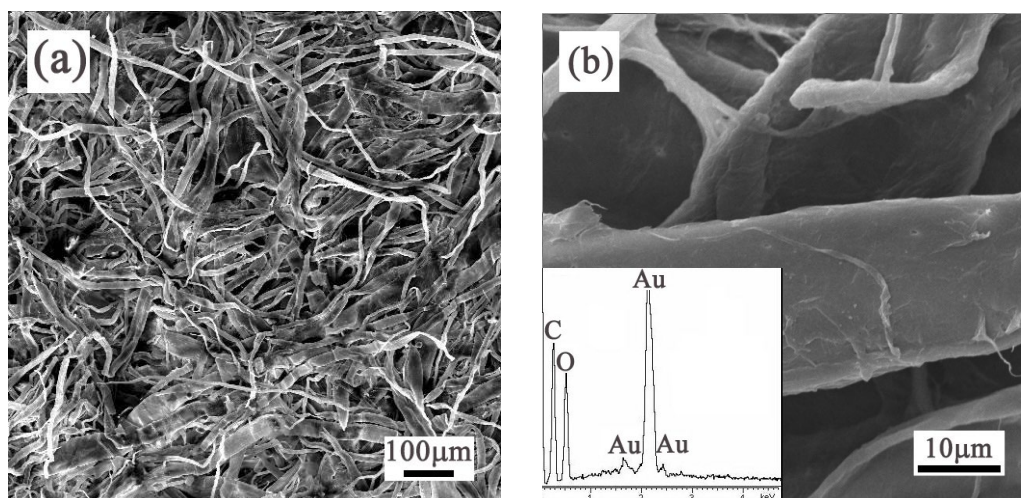


Fig. 3. SEM image of the tissue and its corresponding EDS spectrum.

Table 1. Energy spectrum of the tissue.

Element	App.	Intensity	Weight%	Weight% (Sigma)	Atomic%
C K	37.45	1.1470	44.43	0.99	51.57
O K	26.84	0.6577	55.57	0.99	48.43
Totals			100.00		

The XRD patterns of the carbonized and activated tissue were shown in Figure 4. The details of the phase structure and graphitization process of carbon materials were obtained from XRD studies. It revealed that the diffraction peaks were broad and weak, which could be explained why the tissue carbons were mainly amorphous after carbonization and activation. The Raman spectrum could prove this.

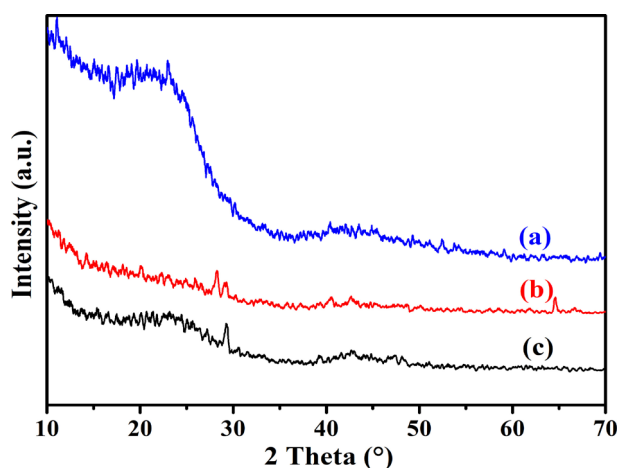


Fig. 4. XRD patterns of tissues after carbonization and activation (a) No activation, (b) Activated by CO_2 at $900\text{ }^\circ\text{C}$ for 2 h, (c) Activated by CO_2 at $900\text{ }^\circ\text{C}$ for 3 h.

The Raman spectra of prepared activated carbon materials were shown in Figure 5. The lines centered around 1600 cm^{-1} and 1350 cm^{-1} were attributed to the Graphitic and Disordered carbon structure. The term “Graphitic” refers to three carbon atoms coordinated and bound by sp^2 type bonding orbitals, independent of layers stacking along the c-direction. The “Disorder” in the carbon sheet may be due to the non-planar microstructural distortions or due to the disorganized regions near the crystal edges. Lattice defects such as edge dislocations and lattice vacancies also contributed to the band at 1350 cm^{-1} . It indicated that the prepared activated carbon materials had a graphitic and amorphous structure, which verified the above XRD analysis.

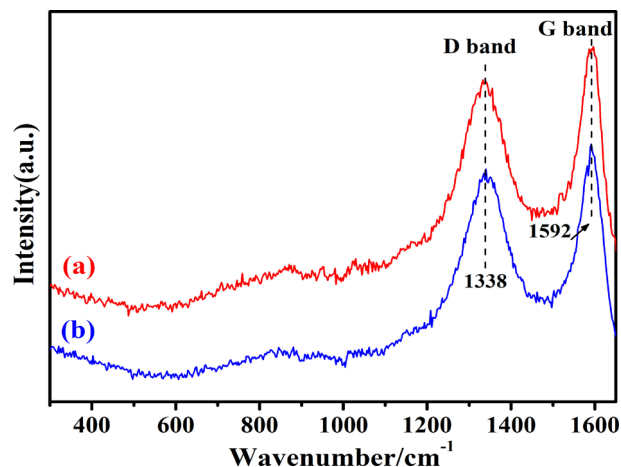


Fig. 5. Raman Spectrum of prepared activated carbon activated by CO_2 at 900°C for (a) 2 h, (b) 3 h.

The SEM was used to investigate the surface topography of activated carbon fibers. Figure 6 showed a typical SEM micrograph of the activated carbon fibers in this paper. The SEM image of the activated carbon fiber (Figure 6(c)) showed that the samples exhibited a fibrous structure that retained the original fibrous structure of the tissue, with a diameter of about $8\mu\text{m}$. High magnification of the fibers displayed that ACFs had lots of mesopores which were confirmed by nitrogen adsorption–desorption isotherm.

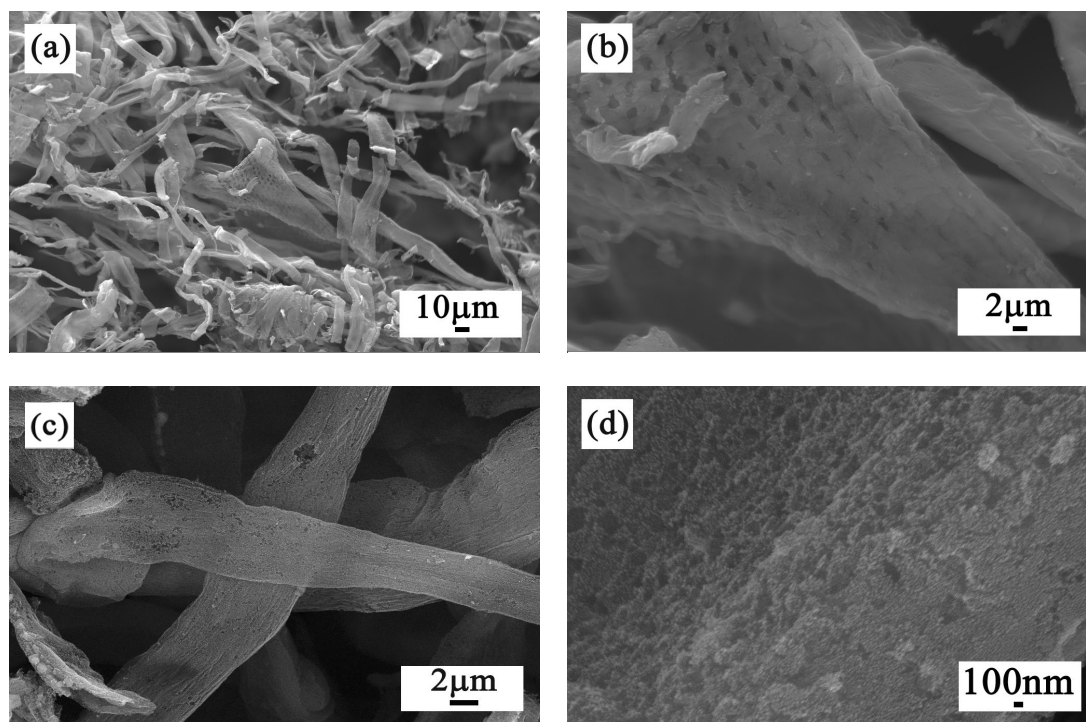


Fig. 6. SEM images of prepared ACFs. (a) Low magnification image of ACFs, (b-d) Magnified image of ACFs.

The texture properties of the produced tissues-based ACFs were given in Table 2. The specific surface areas of the samples activated for 2 and 3 hours were 1517 m²/g and 1474 m²/g, respectively, which were in the range of commercial activated carbon. Furthermore, it was obvious from Table 3 that the tissues-based ACFs obtained by CO₂ activation presented higher BET surface area than those prepared by other methods [23–25]. This indicated that ACFs prepared from tissues by CO₂ would show good adsorption properties.

Figure 7 and Figure 8 showed typical nitrogen adsorption–desorption isotherm and corresponding pore-size distributions curved of samples activated at 900°C by CO₂ for 1 hour, 2 hours, 3 hours, and 4 hours. Careful inspection of the isotherms can provide detailed insight into the type and nature of the pores present in the carbon materials. The prepared activated carbon materials correspond to the type IV isotherms based on BDDT classification [26]. According to the type of isotherm and pore size distribution plots, the activated carbon fibers can be confirmed to be mesoporous materials with an average pore size of 2–5 nm, which was in good agreement with Table 2.

Figure 9 showed that the specific surface area of ACFs decreased from 1517 m²/g to 896 m²/g while prolonging activated time from 2 hours to 4 hours, which could be explained by the increase of carbon and carbon dioxide reflectivity destroyed the concentrated pore size distribution. The best result was activated for 2 h, with a specific surface area of 1517 m²/g, micro surface area of 412.9 m²/g, and total pore volume of 1.194 cm³/g.

Table 2. Textural characteristics of ACFs prepared by CO₂ activation of tissues.

Type of the activated carbon	S _{BET} (m ² /g)	S _{Micro} (m ² /g)	V _T (cm ³ /g)	d(nm)
Activation for 1 h	122	19.4	0.092	5.031
Activation for 2 h	1517	412.9	1.194	3.147
Activation for 3 h	1474	304.1	1.297	3.518
Activation for 4 h	896	549.6	0.562	4.179

S_{micro}: Micropore area deduced from *t*-plot; *V_T*: Total pore volume; *d*: Mean pore diameter, $d=4V/A$ (in nm), where *V* was the total pore volume and *A* was the BET specific surface area.

Table 3. The SBET of Tissues-based ACFs produced by CO₂ and other ACFs.

Sample	Activating Agent	Activation Temperature (°C)	Activation Time (min)	S _{BET} (m ² /g)
Tissues-based ACFs-2h	CO ₂	900	120	1517
Tissues-based ACFs-3h	CO ₂	900	180	1474
ZACF-700 ^a	ZnCl ₂	700	60	1086
ACF-900WB ^b	Steam	900	60	1482
WACFs-900 ^c	CO ₂	900	40	560
ACF-1~3 ^d	KOH	850	60	536~1371

^a: MA et al. (2019), ^b: ZHANG et al. (2013), ^c: LI et al. (2013), ^d: HUANG et al. (2016).

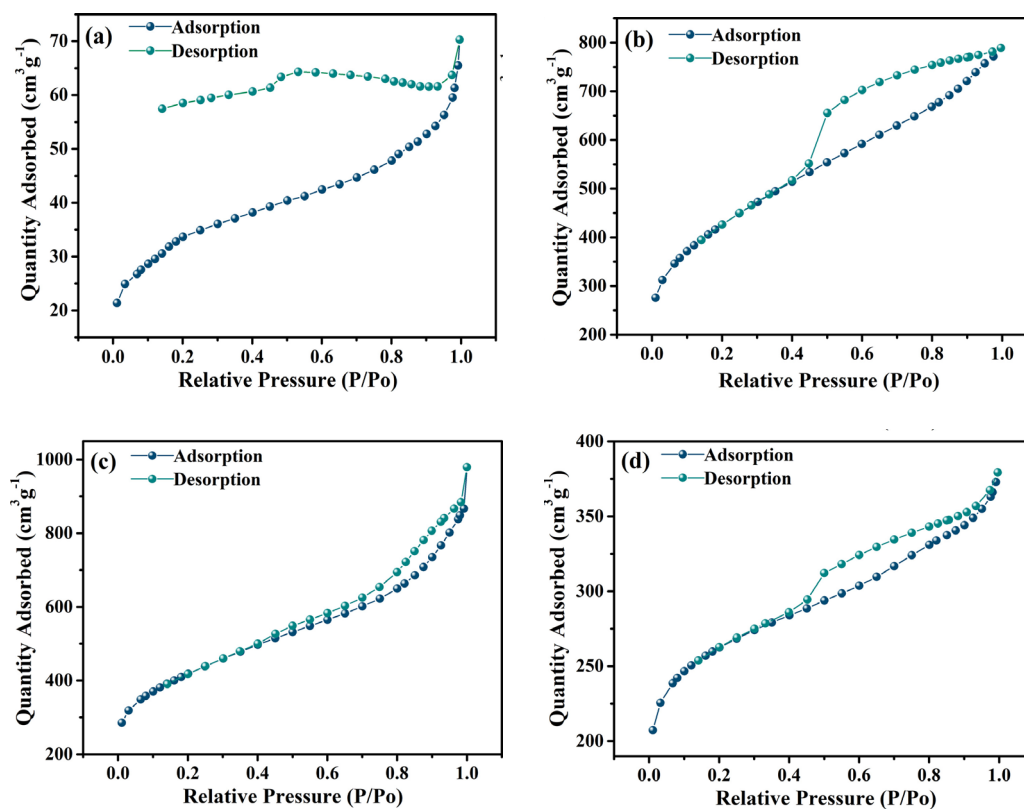


Fig. 7. Nitrogen adsorption-desorption isotherms of the samples activated with CO_2 at $900\text{ }^\circ\text{C}$ for (a) 1h, (b) 2h, (c) 3h, (d) 4h.

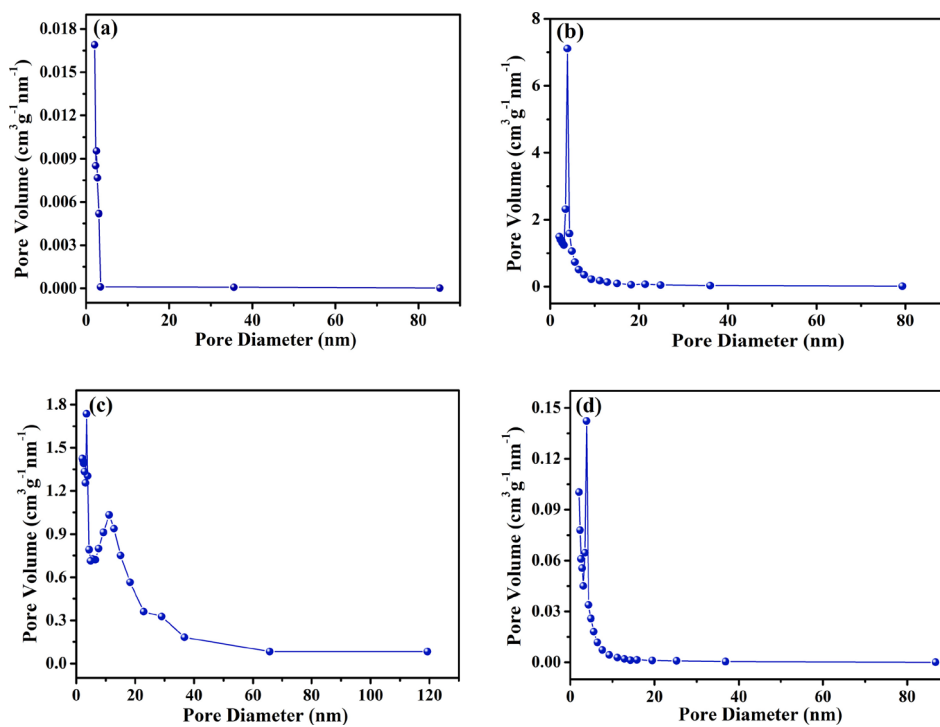


Fig. 8. Pore size distribution plots of the infiltrated samples activated with CO_2 at $900\text{ }^\circ\text{C}$ for (a) 1h, (b) 2h, (c) 3h, (d) 4h.

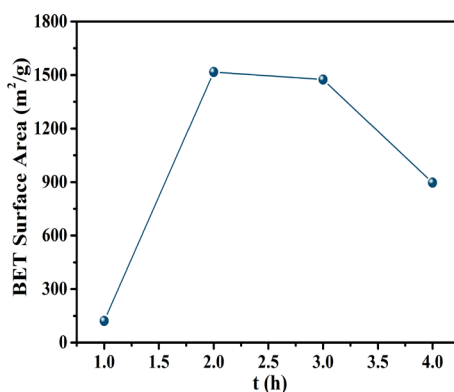


Fig. 9. SBET of ACFs prepared by CO₂ at 900 °C at different activated time

3.2 Adsorption kinetic models of ACFs

To evaluate the kinetic mechanism that controlled the adsorption process, the pseudo-first-order[27], pseudo-second-order[28], and intraparticle diffusion[29] were tested to interpret the experimental data. The above three kinetic mechanisms were, respectively, expressed as the following equations:

$$\frac{1}{q_t} = \frac{1}{q_e} + \frac{k_1}{q_e} \left(\frac{1}{t}\right) \quad (1)$$

where t was the adsorption time, q_t was the adsorption at time t , K_1 was the constant, and q_e was the equilibrium adsorption.

$$\frac{t}{q_t} = \frac{1}{K_2 q_e^2} + \frac{t}{q_e} \quad (2)$$

where t was the adsorption time, q_t as the adsorption at time t , K_2 was the constant, and q_e was the equilibrium adsorption.

$$q_t = k_p t^{1/2} + C \quad (3)$$

where t was the adsorption time, q_t was the adsorption at time t , K_p was the constant, and C was the intercept.

Figure 10 showed three kinetic models for the removal of MB by adsorption on the prepared activated carbon fibers. In this paper, the adsorption data of the samples agree better with Eq.(2) than the others, implying that physical adsorption rather than chemical adsorption occurred during the adsorption process. Kinetic parameters for the adsorption of methylene blue onto the ACFs at room temperature were given in Table 4. The MB adsorption onto the ACFs from the tissue followed the pseudo-second-order rate model well, with the correlation coefficients higher than 0.998 for all samples in this paper. The equilibrium adsorption capacities of ACFs were 526 mg/g and 469 mg/g respectively after activation for 2 hours and 3 hours.

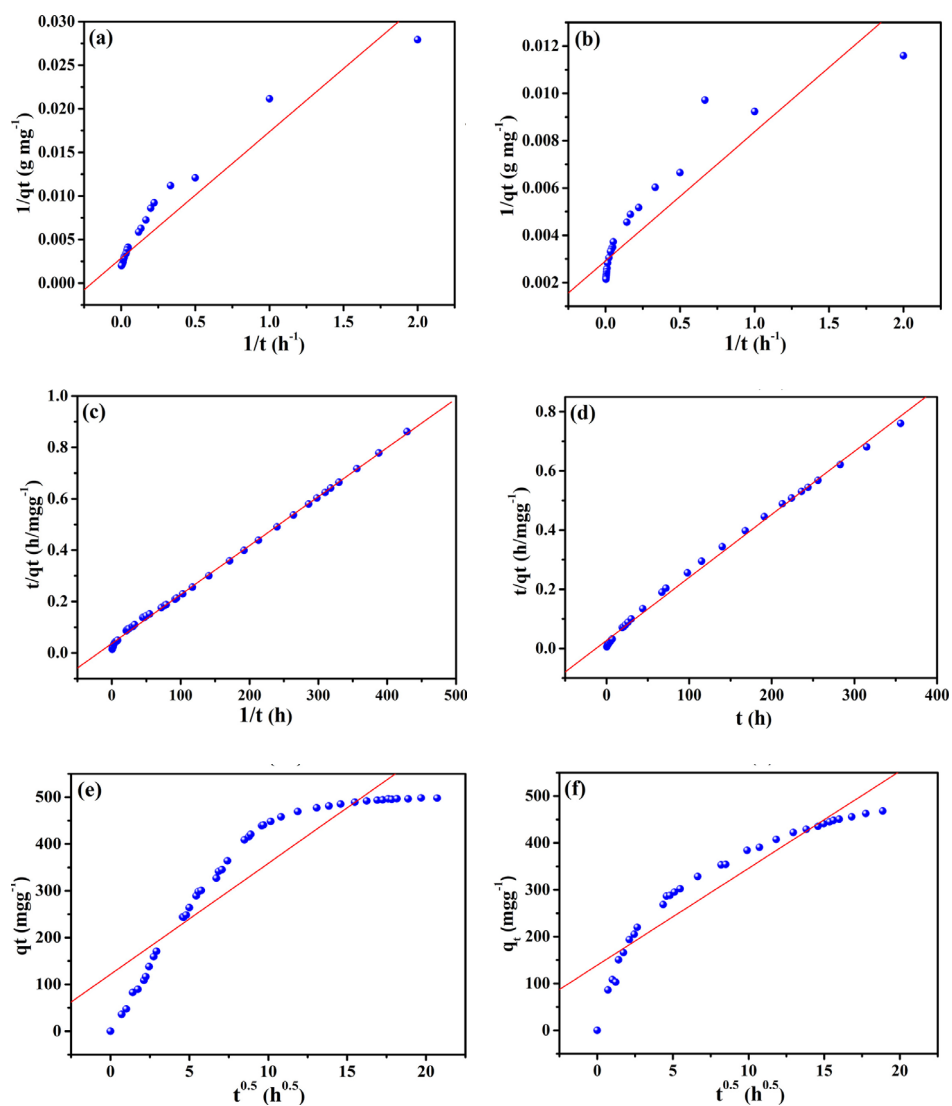


Fig. 10. Three kinetic models for the removal of MB by adsorption on the prepared activated carbon fibers. Pseudo-first-order kinetics for ACFs (a) Activation for 2 h, (b) Activation for 3 h. Pseudo-second-order kinetics for ACFs (c) Activation for 2 h, (d) Activation for 3 h. Intraparticle diffusion kinetics for ACFs (e) Activation for 2 h, (f) Activation for 3 h.

Table 4. Kinetic parameters for the adsorption of MB onto ACFs at room temperature.

Pseudo-first-order	Activation for 2 h	Activation for 3 h
K_l (h^{-1})	5.071	1.873
q_e (mg/g)	349.3	342.5
R	0.9599	0.9176
Pseudo-second-order	Activation for 2 h	Activation for 3 h
K_l (h^{-1})	0.981×10^{-4}	1.723×10^{-4}
q_e (mg/g)	526.3	469.4
R	0.9994	0.9982

4. Conclusions

Tissues were used as raw materials for the production of activated carbon fibers using carbon dioxide as activators. The chemical properties of the resulting ACFs and their liquid phase adsorption properties were investigated. The SEM results indicated that the sample retained a fibrous structure with lots of mesopores. The N₂ adsorption/desorption isotherms indicated that CO₂ activation provided ACFs with a large surface area and a well-developed porosity. The obtained best result was activation for 2 h, with a specific surface area of 1517 m²/g, micro surface area of 412.9 m²/g, and total pore volume of 1.194 cm³/g, which was in the range of commercial activated carbon fibers.

The kinetic model of the Pseudo-second-order equation was more suitable for MB adsorption onto ACFs than the Pseudo-first-order equation and Intraparticle diffusion kinetics. The adsorption rate of Pseudo-second-order kinetics has a high correlation coefficient value ($R > 0.999$). The maximum adsorption capacity at equilibrium was 526 mg/g. It was supposedly due to the porous character and structure that hist can provide new ideas for the manufacture of high-efficient adsorbents, meanwhile being good for achieving net-zero emissions over the coming decades by CO₂ cycle in the CO₂ activation process.

Acknowledgments

This work was financially supported by the Anhui Provincial Key Research and Development Plan of China (202103a07020017).

References

- [1] B. Liu, C. Du, J.J. Chen, J.Y. Zhai, Y. Wang, H.L. Li, *Chemical Physics Letters* 771,138535(2021); <https://doi.org/10.1016/j.cplett.2021.138535>
- [2] Y.H. Wu, R. Yao, X.Y Zhang, B. Zhang, T.H. Wang, *Journal of Environmental Chemical Engineering* 9,105164(2021); <https://doi.org/10.1016/j.jece.2021.105164>
- [3] M. Lewoyehu, *Journal of Analytical and Applied Pyrolysis* 159,105279(2021); <https://doi.org/10.1016/j.jaap.2021.105279>
- [4] N. Yusof, D. Rana, A.F. Ismail, T. Matsuuraca, *Journal of Applied Research and Technology* 14(1),54(2016); <https://doi.org/10.1016/j.jart.2016.02.001>
- [5] X.F. Zhao, S.Q. Lai, H.X. Liu, L.J. Gao, *Environmental Sciences Supplement* 21,S121 (2009); [https://doi.org/10.1016/S1001-0742\(09\)60053-X](https://doi.org/10.1016/S1001-0742(09)60053-X)
- [6] Y. Yoshikawa, K. Teshima, R. Futamura, H. Tanaka, A.V. Neimark, K. Kaneko, *Journal of Colloid and Interface Science* 578,422 (2020); <https://doi.org/10.1016/j.jcis.2020.06.002>
- [7] N. Saeidi, M.N. Lotfollahi, *Fibers and Polymers* 16(3), 543(2015); <https://doi.org/10.1007/s12221-015-0543-6>
- [8] R.K. Ma, X.X. Qin, Z.G. Liu, Y.L. Fu, *Materials* 12(9),1377 (2019); <https://doi.org/10.3390/ma12091377>
- [9] M. Kwiatkowski, *Journal of Mathematical Chemistry* 55,1893(2017);

<https://doi.org/10.1007/s10910-017-0768-2>

- [10] L. Zhang, L.Y. Tu, Y. Liang, Q. Chen, Z.S. Li, C.H. Li, Z.H. Wang, W. Li, RSC Advances 8(74),42280(2018); <https://doi.org/10.1039/C8RA08990F>
- [11] R. Du, Z.F.Tong, C. Wei, A.M.Qin, G.G. Zhang, International Journal of Electrochemical Science 12(6), 5581(2017); <https://doi.org/10.20964/2017.06.40>
- [12] J. Beak, H.M. Lee, K. H. An, B.J. Kim, Carbon Letters 29,393(2019); <https://doi.org/10.1007/s42823-019-00042-y>
- [13] R. Tamilarasan, R. Tamilarasan, M. Kumar, V. Chithambaram, Digest Journal of Nanomaterials and Biostructures 17(4),1369(2022); <https://doi.org/10.15251/DJNB.2022.174.1369>
- [14] J. Li, F. L. Kwong, D.H.L. NG, Journal of the American Ceramic Society 91(4),1350(2008); <https://doi.org/10.1111/j.1551-2916.2008.02276.x>
- [15] N. Yalcin, V. Sevinc, Carbon 38(14), 1943(2000); [https://doi.org/10.1016/S0008-6223\(00\)00029-4](https://doi.org/10.1016/S0008-6223(00)00029-4)
- [16] O. Baytar, A.A.Ceyhanb, O. Sahina, International Journal of Phytoremediation 23(7), 693(2021); <https://doi.org/10.1080/15226514.2020.1849015>
- [17] P. Alvarez, C. Blanco, M. Granda, Journal of Hazardous Materials 144(1-2),400(2007); <https://doi.org/10.1016/j.jhazmat.2006.10.052>
- [18] Z.J. Zhang, J. Li, F.S. Sun, D.H.L. Ng, F.L Kwong, S.Q. Liu, Chinese Journal of Chemical Physics 24(1),103(2011); <https://doi.org/10.1088/1674-0068/24/01/103-108>
- [19] X.Z. Lan, X. Jiang, Y.H. Song, X.P. Jing, X.D. Xing, Green Process Synth 8,837 (2019); <https://doi.org/10.1515/gps-2019-0054>
- [20] Y.C. Chiang, C. Y. Yeh, C. H. Weng, Applied Sciences 9(10), 1977 (2019); <https://doi.org/10.3390/app9101977>
- [21] A. Sharma, J. Jindal, A. Mittal, K. Kumari, S. Maken, N. Kumar, Environmental Chemistry Letters 19,875(2021); <https://doi.org/10.1007/s10311-020-01153-z>
- [22] Y.C. Chiang, W.T. Chin, C.C. Huang, Polymers 13, 3275(2021); <https://doi.org/10.3390/polym13193275>
- [23] J.H. Zhang, W.B. Zhang, Materials Letters 112, 26(2013); <http://dx.doi.org/10.1016/j.matlet.2013.08.103>
- [24] D.N. Li, X.J. Ma, Cellulose 20,1649(2013); <https://doi.org/10.1007/s10570-013-9981-8>
- [25] Y. Huang, G. Zhao, Holzforschung 70(3), 195(2016); <https://doi.org/10.1515/hf-2015-0051>
- [26] S. Brunater, L.S. Deming, W.E. Deming, E. Teller, Journal of the American Chemical Society 62(7),1723 (1940); <https://doi.org/10.1021/ja01864a025>
- [27] N. Kannan, M.M. Sundaram, Dyes and Pigments 5(1),25(2001); [https://doi.org/10.1016/S0143-7208\(01\)00056-0](https://doi.org/10.1016/S0143-7208(01)00056-0)
- [28] Y.S. Ho, G. Mckay, Process Safety and Environmental Protection 76(2), 183(1998); <https://doi.org/10.1205/095758298529326>
- [29] J.W.J. Weber, J.C. Morris, Journal of Saint, Engineering Division of American Society of Civil Engineers 89(1) ,53(1963).